

# Provable Surface Reconstruction from Noisy Samples \*

Tamal K. Dey

Dept. Computer Science & Engineering  
The Ohio State University, USA  
tamaldey@cse.ohio-state.edu

Samrat Goswami

Dept. Computer Science & Engineering  
The Ohio State University  
goswami@cse.ohio-state.edu

## Abstract

We present an algorithm for surface reconstruction in presence of noise. We show that, under a reasonable noise model, the algorithm has theoretical guarantees. Actual performance of the algorithm is illustrated by our experimental results.

## 1 Introduction

The problem of surface reconstruction asks to approximate a surface from a set of point samples. This problem has been the focus of research across many fields because of its wide applications. A number of algorithms, though not with any theoretical guarantees, have been proposed for the problem [1, 6, 7, 18, 20, 21]. Recently, a class of algorithms, following the work of Amenta and Bern [2], have been designed that provide theoretical guarantees [3, 4, 8, 12, 15]. These theoretical guarantees are based on the fact that the input sample is dense with respect to the *local feature size*. However, in practice, this condition may not hold. There are several reasons for this undersampling [12]. Of particular interest is the presence of noise that is typical for samples obtained by a scanning process. Algorithms for curve reconstruction [10] and surface normal estimations [24] from noisy samples have been designed. Also, some of the existing surface reconstruction algorithms work well in presence of noise [4, 13, 22]. Until the conference version of this paper, there was no known algorithm with theoretical guarantees for surface reconstruction in presence of noise. In a simultaneous work, Cheng and Poon [11] extended the curve reconstruction algorithm for noisy samples [10] to three dimensions. This algorithm is significantly different from ours and works on a weaker noise

model. We also believe that the algorithm presented in this paper is more practical.

We prove the theoretical guarantees of our algorithm under some reasonable noise model. The model allows the points to be scattered around the sampled surface and the range of the scatter is restricted by the local feature size. The algorithm works with the Delaunay/Voronoi diagrams of the input points and draws upon some of the principles of the power crust algorithm [4]. In the power crust algorithm it is observed that the union of a set of Delaunay balls called polar balls approximates the solid bounded by the sampled surface. Obviously, this property does not hold in presence of noise. Nevertheless, we observe that, under the assumed noise model, some of the Delaunay balls are relatively big and can play the role of the polar balls. These balls are identified and partitioned into inner and outer balls. We show that the boundary of the union of the outer (or inner) big Delaunay balls is homeomorphic to the sampled surface. This immediately gives a homeomorphic surface reconstruction though the reconstructed surface may not interpolate the sample points.

We extend the algorithm further to compute a homeomorphic surface interpolating a subset of the input sample points. These points reside on the outer (or inner) big Delaunay balls. The rest of the points are deleted. We show that the Delaunay triangulation of the chosen sample points restricted to the boundary of the chosen big Delaunay balls is homeomorphic to the sampled surface. Figure 1 illustrates this algorithm.

## 2 Preliminaries

### 2.1 Definitions

For a set  $Y \subseteq \mathbb{R}^3$  and a point  $x \in \mathbb{R}^3$ , let  $d(x, Y)$  denote the Euclidean distance of  $x$  from  $Y$ ; that is,

$$d(x, Y) = \inf_{y \in Y} \{\|x - y\|\}.$$

---

\*Research partly supported by NSF CARGO grants DMS-0310642, DMS-0138456 and ARO grant DAAD19-02-1-0347.

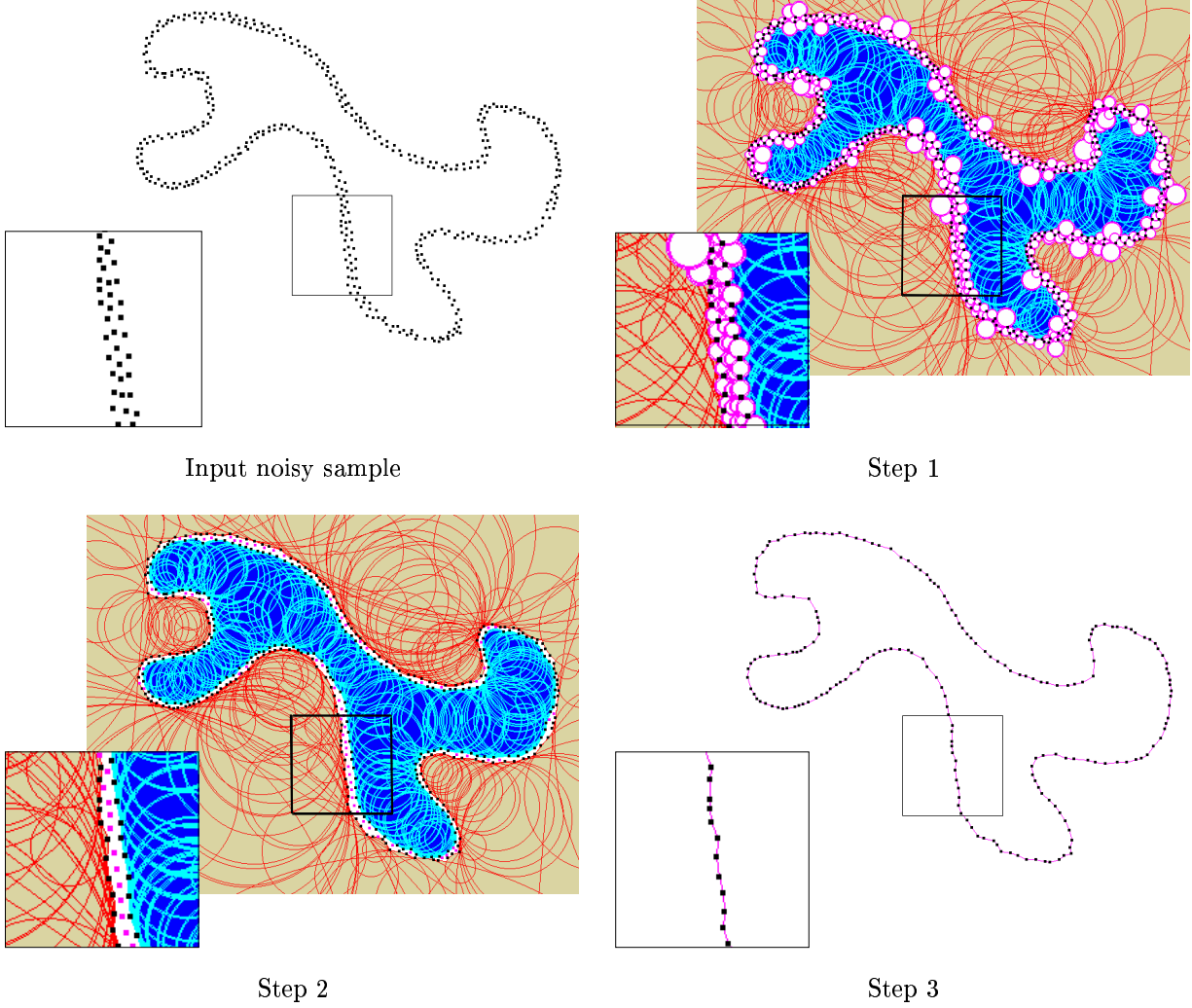


Figure 1: Step 1: Big Delaunay balls (shaded) are separated from small ones (unshaded), Step 2: Outer and inner big Delaunay balls are separated, Step 3: Only the points on the outer balls are retained and the curve (surface) is reconstructed from them.

The set  $B_{r,c} = \{y \in \mathbb{R}^3, \|y - c\| \leq r\}$  is a *ball* with radius  $r$  and center  $c$ .

*Voronoi and Delaunay diagram.* For a finite point set  $P \subset \mathbb{R}^3$ , the Voronoi diagram  $\text{Vor } P$  is the collection of *Voronoi faces* defined as follows. The *Voronoi cell* for a point  $p \in P$  is

$$V_p = \{x \in \mathbb{R}^3 \mid d(x, P) = \|x - p\|\}.$$

Closed faces shared by  $d$  Voronoi cells,  $1 \leq d \leq 4$ , are called  $(4 - d)$ -dimensional Voronoi faces. The 0-, 1-, 2-, 3-dimensional Voronoi faces are called *Voronoi vertices, edges, facets* and *cells* respectively.

The *Delaunay diagram* of  $P$  is a dual to  $\text{Vor } P$ . The convex hull of  $d \leq 4$  points defines a  $(d - 1)$ -dimensional *Delaunay face* if the intersection of their corresponding Voronoi cells is not empty. If the points are in general position 1-, 2-, 3-dimensional Delaunay faces are *Delaunay edges, triangles and tetrahedra* respectively. They define a decomposition of the convex hull of all points in  $P$  called the *Delaunay triangulation*  $\text{Del } P$ . We assume general positions.

*Sampled surface.* Let  $\Sigma \subset \mathbb{R}^3$  be a compact smooth surface without boundary from which the input sample is derived possibly with noise. Also, we assume that  $\Sigma$  is connected.

The *medial axis*  $M$  of  $\Sigma$  is the closure of the set  $Y$  so that, for each  $y \in Y$ ,  $d(y, \Sigma)$  is realized by two or more points of  $\Sigma$ . In other words, each point  $y \in M$  is the center of a maximal ball whose interior is empty of points from  $\Sigma$ . This ball meets  $\Sigma$  only tangentially. We call each such ball  $B_{r,y}$  a *medial ball* where  $r = d(y, \Sigma)$ . For each point  $x \in \Sigma$ , consider a function  $f : \Sigma \rightarrow \mathbb{R}$  where  $f(x) = d(x, M)$ . Except for some pathological cases,  $f(x)$  is strictly positive for smooth surfaces. The function  $f(\cdot)$ , also called the *local feature size*, satisfies the following Lipschitz property [2].

*Lipschitz property.* For any two points  $x, y \in \Sigma$ ,  $f(x) \leq f(y) + \|x - y\|$ .

## 2.2 Sampling

A finite set of points  $P \subset \Sigma$  is called an  $\varepsilon$ -*sample* of  $\Sigma$  if

$$d(x, P) \leq \varepsilon d(x, M) \quad \text{for each } x \in \Sigma.$$

We consider a noisy sample of  $\Sigma$  which may not be a subset of  $\Sigma$ , but we assume that it lies close to the surface. This proximity assumption alone cannot

disambiguate the reconstruction process as sample points can collaborate to form arbitrary patterns. To prevent this collaboration we incorporate a locally uniform sampling condition.

Let  $\nu : \mathbb{R}^3 \setminus M \rightarrow \Sigma$  map a point  $x \in \mathbb{R}^3$  to the closest point  $\nu(x)$  on  $\Sigma$ . Denote  $\tilde{p} = \nu(p)$  and  $\tilde{P} = \{\nu(p)\}_{p \in P}$ .

*Noise Model.* We say  $P \subset \mathbb{R}^3$  is a  $(\varepsilon, \kappa)$ -*sample* of  $\Sigma$  if the following sampling conditions hold for some small  $\varepsilon > 0$  and a small interger  $\kappa \geq 1$ .

- (i)  $\tilde{P}$  is an  $\varepsilon$ -sample of  $\Sigma$ ,
- (ii)  $\|p - \tilde{p}\| \leq \varepsilon^2 f(\tilde{p})$ ,
- (iii)  $\|p - q\| \geq \varepsilon f(\tilde{p})$  for any two points  $p, q$  in  $P$  where  $q$  is the  $\kappa$ th nearest sample point to  $p$ .

All along we assume that the input  $P$  is a  $(\varepsilon, \kappa)$ -sample of  $\Sigma$  for some suitable  $\varepsilon$  and  $\kappa$ . The first condition of the noise model says that the projection of the point set  $P$  on the surface makes a dense sample and the second one says that  $P$  is close to the surface. The third condition makes the sampling locally uniform. Notice that, for  $\kappa = 1$  this condition prohibits any two sample points to be arbitrarily close. But, that may be a severe restriction for point samples in practice. This is why we introduce  $\kappa$  to make the locally uniform condition less restrictive. This condition is very similar to the locally uniform conditions used in [15]. In practice we take  $\kappa$  in the range of three to five.

*Sampling parameters.* In the sequel we will formulate and use several  $\varepsilon_i > 0$ ,  $i = 1, \dots, 9$  which have the property that  $\lim_{\varepsilon \rightarrow 0} \varepsilon_i = 0$ .

Some of the immediate consequences of the sampling requirements are the following lemmas.

**Lemma 1** *Any point  $x \in \Sigma$  has a sample point within  $\varepsilon_1 f(x)$  distance where  $\varepsilon_1 = \varepsilon(1 + \varepsilon + \varepsilon^2)$ .*

PROOF. From the sampling condition (i), we must have a sample point  $p$  so that  $\|x - \tilde{p}\| \leq \varepsilon f(x)$ . Also,  $\|p - \tilde{p}\| \leq \varepsilon^2 f(\tilde{p}) \leq \varepsilon^2(1 + \varepsilon)f(x)$ . Thus,

$$\begin{aligned} \|x - p\| &\leq \|x - \tilde{p}\| + \|\tilde{p} - p\| \\ &\leq \varepsilon f(x) + \varepsilon^2(1 + \varepsilon)f(x) \\ &\leq \varepsilon(1 + \varepsilon + \varepsilon^2)f(x). \end{aligned}$$

□

**Lemma 2** Any sample point  $p \in P$  has its  $\kappa$ th closest sample point within  $\varepsilon_2 f(\tilde{p})$  distance where

$$\varepsilon_2 = \left( \varepsilon + \frac{4\kappa + \varepsilon}{1 - 4\kappa\varepsilon} \right) \varepsilon.$$

PROOF. Consider the locally uniform sample  $\tilde{P}$ . It is an easy consequence of the sampling condition (i) and the Lipschitz property of  $f(\cdot)$  that, for each  $x \in \Sigma$  there exists a sample point  $p$  so that  $\|\tilde{p} - x\| \leq \frac{\varepsilon}{1-\varepsilon} f(\tilde{p})$ . This means that, for sufficiently small  $\varepsilon$ , balls of radius  $2\varepsilon f(\tilde{p}) > \frac{\varepsilon}{1-\varepsilon} f(\tilde{p})$  around each point  $\tilde{p} \in \tilde{P}$  cover  $\Sigma$ . Consider the graph where a point  $\tilde{p} \in \tilde{P}$  is joined with  $\tilde{q} \in \tilde{P}$  with an edge if the balls  $B_{r_1, \tilde{p}}$  and  $B_{r_2, \tilde{q}}$  intersect where  $r_1 = 2\varepsilon f(\tilde{p})$  and  $r_2 = 2\varepsilon f(\tilde{q})$ . Consider a simple path  $\Pi$  of  $\kappa$  edges in this graph with one endpoint at  $\tilde{p}$ . An edge between two points  $\tilde{p}$  and  $\tilde{q}$  in the graph has a length at most  $2\varepsilon(f(\tilde{p}) + f(\tilde{q}))$ . The path  $\Pi$  thus has length at most

$$\ell = 2\varepsilon(f(\tilde{p}) + 2f(\tilde{q}_1) + \dots + 2f(\tilde{q}_{\kappa-1}) + f(\tilde{q}_\kappa))$$

where  $\tilde{q}_i, i = 1, \dots, \kappa$  are the vertices ordered along the path. Denoting  $f_{max}$  as the maximum of the feature sizes of all vertices on the considered path we get

$$\begin{aligned} \ell &\leq 4\kappa\varepsilon f_{max} \\ &\leq \frac{4\kappa\varepsilon}{1 - 4\kappa\varepsilon} f(\tilde{p}). \end{aligned}$$

The distance from  $p$  to the farthest point, say  $q$ , among the  $\kappa$  closest points to  $p$  cannot be more than the length of  $\Pi$  and thus is within distance

$$\begin{aligned} d &\leq \|p - \tilde{p}\| + \|\tilde{p} - \tilde{q}\| + \|\tilde{q} - q\| \\ &\leq \varepsilon^2 f(\tilde{p}) + \frac{4\kappa\varepsilon}{1 - 4\kappa\varepsilon} f(\tilde{p}) + \frac{\varepsilon^2}{1 - 4\kappa\varepsilon} f(\tilde{p}). \end{aligned}$$

We have  $d \leq \varepsilon_2 f(\tilde{p})$ .  $\square$

### 2.3 Offset surfaces

Many standard arguments used in proving the guarantees of the surface reconstruction algorithms [2, 3, 8] cannot be applied here because  $P$  may not be a subset of  $\Sigma$ . We take the help of offset surfaces of  $\Sigma$  to overcome this difficulty.

Let  $\Omega_O$  denote the unbounded component of  $\mathbb{R}^3 \setminus \Sigma$ . Further, let  $\Omega_I$  be  $\mathbb{R}^3 \setminus \Omega_O$ . Notice that, by our definition,  $\Omega_I$  is closed where  $\Omega_O$  is open and  $\mathbb{R}^3 = \Omega_I \cup \Omega_O$ . The definition of offset surfaces

and subsequent proofs require an orientation of the normals of  $\Sigma$ . We orient the normal  $\mathbf{n}_x$  at any point  $x \in \Sigma$  so that it points locally outside, i.e., towards  $\Omega_O$ . Consider the signed distance function

$$h : \mathbb{R}^3 \rightarrow \mathbb{R} \text{ where } h(x) = (x - \tilde{x}) \cdot \mathbf{n}_{\tilde{x}}.$$

This function is smooth everywhere except at the medial axis  $M$ . We consider two level sets avoiding the medial axis. Let

$$\Sigma_{-\varepsilon} = \{x \in \mathbb{R}^3 \mid |h(x)| = 3\varepsilon^2 f(\tilde{x}) \text{ and } h(x) < 0\}$$

and

$$\Sigma_{+\varepsilon} = \{x \in \mathbb{R}^3 \mid |h(x)| = 3\varepsilon^2 f(\tilde{x}) \text{ and } h(x) > 0\}.$$

The offset surfaces are not necessarily smooth. The reason is that the function  $f$  is not necessarily smooth though they are continuous. Contrast this property of  $\Sigma_{-\varepsilon}$  and  $\Sigma_{+\varepsilon}$  with the offset surfaces defined by small constant offsets which are necessarily smooth. The definitions of  $\Sigma_{-\varepsilon}$  and  $\Sigma_{+\varepsilon}$  are motivated by our noise model. This noise model allows the points to lie in a band of width proportional to the local feature sizes. This is less restrictive than allowing them to lie within a band of constant width. The particular choice of the factor  $3\varepsilon^2$  in defining the offset surfaces is motivated by the result of Lemma 4.

The two offset surfaces  $\Sigma_{-\varepsilon}, \Sigma_{+\varepsilon}$  enjoy some nice properties.

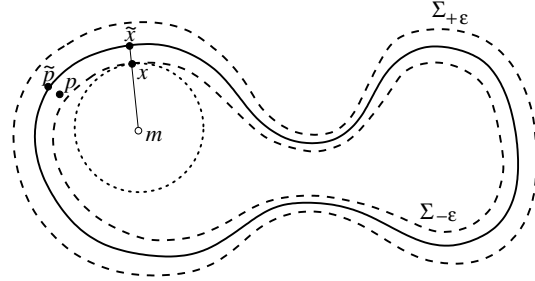


Figure 2: A point  $x$  on the offset surface  $\Sigma_{-\varepsilon}$  has its closest point  $\nu(x) = \tilde{x}$  on  $\Sigma$ . The feature ball centering  $m$  and touching  $\Sigma_{-\varepsilon}$  at  $x$  is shown with the dotted boundary. The points  $x, \tilde{x}$  and the point  $m$  are collinear.

**Lemma 3** For sufficiently small  $\varepsilon$ , the surfaces  $\Sigma_{-\varepsilon}$  and  $\Sigma_{+\varepsilon}$  are homeomorphic to  $\Sigma$ . Also, any point  $x$  on either  $\Sigma_{-\varepsilon}$  or  $\Sigma_{+\varepsilon}$  has  $\tilde{x}$  within  $\varepsilon_3 f(\tilde{x})$  distance and a sample point within  $\varepsilon_4 f(\tilde{x})$  distance where  $\varepsilon_3 = 3\varepsilon^2$  and  $\varepsilon_4 = (\varepsilon_1 + 3\varepsilon^2)$ .

PROOF. Consider the map  $\nu$  defined earlier which associates a point  $x \in \mathbb{R}^3$  to its closest point  $\tilde{x}$  on  $\Sigma$ . We show that the restriction  $\nu_\varepsilon : \Sigma_{-\varepsilon} \rightarrow \Sigma$  of  $\nu$  is a homeomorphism. The case for  $\Sigma_{+\varepsilon}$  can be proved similarly. First, notice that  $\nu_\varepsilon$  is well defined as  $\Sigma_{-\varepsilon}$  avoids the medial axis. It is continuous as  $\nu$  is so everywhere except at the medial axis. Next, we argue that  $\nu_\varepsilon$  is onto, i.e.,  $\nu_\varepsilon(\Sigma_{-\varepsilon}) = \Sigma$ . This follows almost immediately from the definition of  $\Sigma_{-\varepsilon}$  since for any point  $y \in \Sigma$ ,  $\nu_\varepsilon^{-1}(y)$  is defined as the point  $x \in \mathbb{R}^3$  where  $h(x) = -3\varepsilon^2 f(y)$ . Next, we show that  $\nu_\varepsilon$  is one-to-one. Suppose not. Then, there are two points  $x$  and  $x'$  in  $\Sigma_{-\varepsilon}$  where  $\nu_\varepsilon(x) = \nu_\varepsilon(x') = y$ . It follows that  $x, x'$  and  $y$  are collinear and lie on the line normal to  $\Sigma$  at  $y$ . But, then by definition of  $\Sigma_{-\varepsilon}$ ,  $h(x) = h(x') = -3\varepsilon^2 f(y)$ . This can happen only when  $x = x'$ . The only thing remains to be shown is that  $\nu_\varepsilon^{-1}$  is continuous. Continuity of  $\nu_\varepsilon^{-1}$  follows from the fact that both  $h$  and  $f$  are continuous. This completes the proof that  $\nu_\varepsilon$  is indeed a homeomorphism.

Let  $x$  be any point on  $\Sigma_{-\varepsilon}$ . The proof for the case when  $x \in \Sigma_{+\varepsilon}$  is similar. It follows from the definition that  $\|x - \tilde{x}\| \leq 3\varepsilon^2 f(\tilde{x})$ . The point  $\tilde{x}$  has a sample point within  $\varepsilon_1 f(\tilde{x})$  distance (Lemma 1). Combining the two distance bounds we get the required bound.  $\square$

From this point onward we consider  $\Sigma_{-\varepsilon}$  in all definitions and lemmas. It should be clear that they also hold for  $\Sigma_{+\varepsilon}$ . We introduce the notion of *feature balls* (Figure 2) which will play an important role in the proofs.

**Definition 1** For a point  $x \in \Sigma_{-\varepsilon}$  let  $B_{r,m}$  be the ball with the following conditions:

- $m \in \Omega_I$ ; the boundary of  $B_{r,m}$  meets  $\Sigma_{-\varepsilon}$  at  $x$ ,
- the radius  $r$  is  $(1 - 3\varepsilon^2)f(\tilde{x})$ , and
- the center  $m$  lies on the line of normal at  $\tilde{x}$ . In other words,  $\tilde{m} = \tilde{x}$ .

Call  $B_{r,m}$  the feature ball meeting  $\Sigma_{-\varepsilon}$  at  $x$ .

**Lemma 4** For any point  $x \in \Sigma_{-\varepsilon}$  the interior of the feature ball meeting  $\Sigma_{-\varepsilon}$  at  $x$  is empty of points from  $P$ .

PROOF. Let  $B = B_{r,m}$  be such a feature ball and  $p$  be any point in  $P$  (Figure 2). Observe that

$\|m - \tilde{x}\| = \|m - x\| + \|x - \tilde{x}\| = f(\tilde{x})$ . We have

$$\begin{aligned} f(\tilde{p}) &\leq f(\tilde{x}) + \|\tilde{x} - \tilde{p}\| \\ &\leq f(\tilde{x}) + \|m - \tilde{x}\| + \|m - \tilde{p}\| \\ &\leq 2f(\tilde{x}) + \|m - \tilde{p}\|. \end{aligned}$$

Then,

$$\begin{aligned} \|m - p\| &\geq \|m - \tilde{p}\| - \|p - \tilde{p}\| \\ &\geq \|m - \tilde{p}\| - \varepsilon^2 f(\tilde{p}) \\ &\geq \|m - \tilde{p}\| - \varepsilon^2 (2f(\tilde{x}) + \|m - \tilde{p}\|) \\ &= (1 - \varepsilon^2)\|m - \tilde{p}\| - 2\varepsilon^2 f(\tilde{x}) \\ &\geq (1 - 3\varepsilon^2)f(\tilde{x}) \\ &\quad \text{as } \|m - \tilde{p}\| \geq \|m - \tilde{x}\| = f(\tilde{x}) \\ &= \|m - x\|. \end{aligned}$$

Therefore,  $p$  cannot be in the interior of  $B$ .  $\square$

Also, the following observation will be helpful for our proofs. It says that if a ball with two points  $x$  and  $y$  on its boundary is big relative to the feature size of  $\tilde{x}$ , it remains big relative to the feature size of  $\tilde{y}$  if  $x$  and  $y$  are close to  $\Sigma$ . The parameters  $\lambda$  and  $\varepsilon'$  will be close to 1 and  $\varepsilon$  respectively when we use this lemma later.

**Lemma 5** Let  $B = B_{r,c}$  be a ball with two points  $x$  and  $y$  on its boundary where  $\|x - \tilde{x}\| \leq \varepsilon' f(\tilde{x})$ ,  $\|y - \tilde{y}\| \leq \varepsilon' f(\tilde{y})$ . Then,  $r \geq \frac{\lambda(1-\varepsilon')}{1+2\lambda+\varepsilon'} f(\tilde{y})$  given that  $r \geq \lambda f(\tilde{x})$  for  $\lambda > 0$ .

PROOF. We get

$$\begin{aligned} r &\geq \lambda f(\tilde{x}) \\ &\geq \lambda(f(\tilde{y}) - \|\tilde{x} - \tilde{y}\|) \\ &\geq \lambda(f(\tilde{y}) - \|x - \tilde{x}\| - \|x - y\| - \|y - \tilde{y}\|) \\ &\geq \lambda(f(\tilde{y}) - \varepsilon' f(\tilde{x}) - 2r - \varepsilon' f(\tilde{y})) \\ &\geq \lambda((1 - \varepsilon')f(\tilde{y}) - (2 + \frac{\varepsilon'}{\lambda})r) \end{aligned}$$

from which it follows that

$$\begin{aligned} (1 + 2\lambda + \varepsilon')r &\geq \lambda(1 - \varepsilon')f(\tilde{y}) \\ \text{or, } r &\geq \frac{\lambda(1 - \varepsilon')}{1 + 2\lambda + \varepsilon'} f(\tilde{y}). \end{aligned}$$

$\square$

### 3 Union of balls

As we indicated before, our goal is to filter out a subset of points from  $P$  that lie on big Delaunay balls. We do this by choosing Delaunay balls

that are big compared to the distances of the  $\kappa$ th nearest neighbor from the sample points. Let  $\lambda_p$  denote the distance to the  $\kappa$ th nearest neighbor of a sample point  $p \in P$ . For an appropriate constant  $K > 0$ , we define

$\mathcal{B}$  = set of Delaunay balls  $B_{r,c}$  where  $r > K\lambda_p$  for all points  $p \in P$  incident on the boundary of  $B_{r,c}$ .

Since we know that  $\lambda_p \geq \varepsilon f(\bar{p})$  by the sampling condition (iii), we have:

**Observation 1** *Let  $B_{r,c} \in \mathcal{B}$  be a Delaunay ball with  $p \in P$  on its boundary. Then,  $r > K\varepsilon f(\bar{p})$ .*

Since  $\mathbb{R}^3 = \Omega_I \cup \Omega_O$  we can write  $\mathcal{B} = \mathcal{B}_I \cup \mathcal{B}_O$  where  $\mathcal{B}_I$  is the set of balls having their centers in  $\Omega_I$  and  $\mathcal{B}_O$  is the set of balls with their centers in  $\Omega_O$ . We call the balls in  $\mathcal{B}_I$  the *inner* big Delaunay balls and the ones in  $\mathcal{B}_O$  the *outer* big Delaunay balls.

We will filter out those points from  $P$  that lie on the balls in  $\mathcal{B}$ . A decomposition of  $\mathcal{B}$  induces a decomposition on these points, namely

$$\begin{aligned} P_I &= \{p \in P \cap B \mid B \in \mathcal{B}_I\} \text{ and} \\ P_O &= \{p \in P \cap B \mid B \in \mathcal{B}_O\}. \end{aligned}$$

Notice that  $P_I$  and  $P_O$  may not be disjoint and they decompose only the set of points incident to the balls in  $\mathcal{B}$  and not necessarily the set  $P$ .

Next two lemmas are pivotal for later proofs. The first one about normal approximation has been proved by Dey and Sun [16].

**Lemma 6** *Let  $B_{r,c}$  be a Delaunay ball whose boundary contains a sample point  $p \in P$ . Let  $c$  lie in  $\Omega_I$ . If  $r > f(\bar{p})/5$  then the vector  $\vec{pc}$  makes at most  $200\varepsilon$  angle with  $-\mathbf{n}_{\bar{p}}$  when  $\varepsilon$  is sufficiently small.*

**Lemma 7** *For each point  $x \in \Sigma_{-\varepsilon}$  there is a Delaunay ball that enjoys the following properties when  $\varepsilon$  is sufficiently small:*

- (i) *its radius is at least  $\frac{3}{4}(1 - 3\varepsilon^2)f(\bar{x})$ ,*
- (ii) *its boundary contains a sample point  $p \in P_I$  within a distance  $\varepsilon_5 f(\bar{x})$  from  $x$  where  $\varepsilon_5 = \left(\frac{\frac{7}{4}\varepsilon_4}{\frac{1}{4}(1 - 3\varepsilon^2) + \varepsilon_4}\right)^{\frac{1}{2}}(1 - 3\varepsilon^2) = O(\sqrt{\varepsilon})$ .*

**PROOF.** Consider the feature ball  $B = B_{r,m}$  meeting  $\Sigma_{-\varepsilon}$  at  $x$ . By definition,

$$r = (1 - 3\varepsilon^2)f(\bar{x}).$$

We construct the ball as claimed by deforming  $B$  as follows.

**SHRINKING:** Let  $B^{3/4} = B_{3r/4,m}$  be a shrunk copy of  $B$ . The ball  $B$  and hence  $B^{3/4}$  are empty (Lemma 4).

**TRANSLATION:** Translate  $B^{3/4}$  rigidly by moving the center  $m$  along the direction  $\vec{m}\bar{x}$  until its boundary hits a sample point  $p \in P$ . Let this new ball be denoted  $B' = B'_{r',m'}$ , refer to Figure 3.

**DELAUNAY DEFORMATION:** Deform  $B'$  further to a larger Delaunay ball  $B'' = B''_{r'',m''}$  which we show has the claimed properties. The center  $m'$  of  $B'$  belongs to the Voronoi cell  $V_p$  since  $B'$  is empty of points from  $P$ . Move the center  $m'$  of  $B'$  continuously in  $V_p$  always increasing the distance  $\|m' - p\|$  till  $m'$  meets a Voronoi vertex, say  $m''$ , in  $V_p$ . This motion is possible as the distance function from  $p$  reaches its maxima only at the Voronoi vertices.

**OBSERVATION 1.** Let  $x'$  be the closest point to  $x$  on the boundary of  $B'$ . We have

$$\|x' - x\| \leq \varepsilon_4 f(\bar{x}) \quad (3.1)$$

since otherwise there is an empty ball centering  $x$  with radius  $\varepsilon_4 f(\bar{x})$  and thus  $x$  does not have a sample point within  $\varepsilon_4 f(\bar{x})$  distance violating Lemma 3.

**CLAIM 1.**  $\|x - p\| \leq \varepsilon_5 f(\bar{x})$ .

First, we observe that both  $B$  and  $B'$  contain their centers in their intersection. Since  $B'$  has a radius smaller than  $B$ , it is sufficient to show that  $B'$  contains  $m$  inside. During the rigid translation when the ball  $B^{3/4}$  touches  $B$  at  $x$ , its center moves by  $\frac{1}{4}r$  distance. After that, we move  $B^{3/4}$  by the distance  $\|x - x'\| \leq \varepsilon_4 f(\bar{x})$  (Inequality 3.1). Thus,

$$\|m - m'\| \leq \frac{1}{4}r + \varepsilon_4 f(\bar{x}). \quad (3.2)$$

Therefore, the distance between  $m$  and  $m'$  is less than  $\frac{3}{4}r$  for sufficiently small  $\varepsilon$  implying that  $m$  is in  $B'$ .

Now we show the claimed bound for  $\|x - p\|$ . The point  $p$  can only be on that part of the boundary of  $B'$  which is outside the empty ball  $B$ . This with the fact that the centers of  $B$  and  $B'$  are in their intersection imply that the largest distance from  $x$  to  $p$  is realized when  $p$  is on the circle where the

boundaries of  $B$  and  $B'$  intersect. Consider this situation as in Figure 3.

Let  $d = \|m' - m\|$ . First, observe that

$$\frac{1}{4}r \leq d \leq \frac{1}{4}r + \varepsilon_4 f(\tilde{x}). \quad (3.3)$$

The first half of the inequality holds since  $B$  is empty of samples and hence  $B^{\frac{3}{4}}$  has to move out of it to hit a sample point. The second half of the inequality follows from the inequality 3.2. Since

$$\begin{aligned} \|p - q\|^2 &= \|m' - p\|^2 - \|m' - q\|^2 \\ &= \|m - p\|^2 - \|m - q\|^2, \end{aligned}$$

we have

$$\|m' - q\| = \frac{r^2 - (r')^2 - d^2}{2d}.$$

Hence

$$\begin{aligned} \|x - p\|^2 &= \|p - q\|^2 + \|q - x\|^2 \\ &= r^2 - (d + \|m' - q\|)^2 \\ &\quad + (r - (d + \|m' - q\|))^2 \\ &= 2r^2 - rd - \frac{r}{d}(r^2 - r'^2) \\ &\stackrel{\text{Ineq. 3.3}}{\leq} \frac{\varepsilon_4(1 + \frac{3}{4})}{\frac{1}{4}(1 - 3\varepsilon^2) + \varepsilon_4} r^2. \end{aligned}$$

The claimed bound on  $\|x - p\|$  follows immediately.

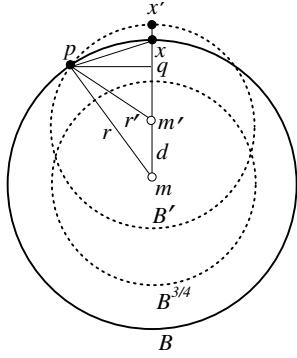


Figure 3: Deformation of  $B$  to  $B'$ .

CLAIM 2.  $m'' \in \Omega_I$ .

To prove this claim we first show that the radius  $r'$  of  $B'$ , which is  $\frac{3}{4}r = \frac{3}{4}(1 - 3\varepsilon^2)f(\tilde{x})$ , is also large compared to  $f(\tilde{p})$ . Observe that  $\|x' - \tilde{x}\|$  is at most  $\varepsilon_4 f(\tilde{x})$  if  $\tilde{x}$  lies between  $x$  and  $x'$  and is at most  $3\varepsilon^2 f(\tilde{x})$  if it does not. Hence  $\|x' - \tilde{x}\| \leq \max\{\varepsilon_4, 3\varepsilon^2\}f(\tilde{x})$ . For sufficiently small  $\varepsilon$ , we have  $\varepsilon_4 > 3\varepsilon^2$ . Therefore, we can say  $\|x' - \tilde{x}\| \leq \varepsilon_4 f(\tilde{x})$ . We know  $\|p - \tilde{p}\| \leq \varepsilon^2 f(\tilde{p})$ . Therefore, we can

apply Lemma 5 with  $\varepsilon' = \varepsilon_4$  and  $\lambda = \frac{3}{4}(1 - 3\varepsilon^2)$  to deduce that  $r' = \|p - m'\| \geq \beta f(\tilde{p})$  where

$$\beta = \frac{3}{10} \frac{(1 - 3\varepsilon^2)(1 - \varepsilon_4)}{1 + O(\varepsilon)}.$$

This means

$$r' \geq \left(\frac{3}{10} - O(\varepsilon)\right)f(\tilde{p}). \quad (3.4)$$

Now we show that the center of  $B'$  cannot reach a point in  $\Sigma$  during its deformation to  $B''$  establishing  $m'' \in \Omega_I$ . Suppose not, i.e., the center of  $B'$  reaches a point  $y \in \Sigma$  during the deformation. Then, we reach a contradiction.

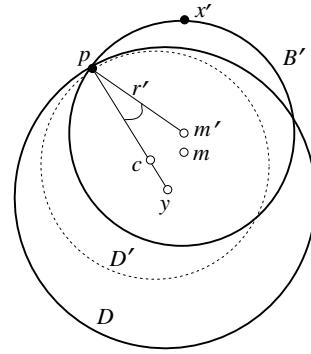


Figure 4: The balls  $B'$  and  $D$  incident to  $p$ . The reduced ball  $D'$  shown with dotted circle contains  $m$ .

First observe that  $m'$  is in  $\Omega_I$  as it is only within  $\frac{1}{4}r + \varepsilon_4 f(\tilde{x})$  distance away from  $m$ . Next, consider the two balls  $B'$  and  $D = B_{\|y-p\|,y}$  meeting at  $p$  (Figure 4). Both have radii larger than  $(\frac{3}{10} - O(\varepsilon))f(\tilde{p})$  (Inequality 3.4) which is at least  $\frac{f(\tilde{p})}{5}$  for sufficiently small  $\varepsilon$ . Both vectors  $\vec{p}\tilde{y}$  and  $\vec{p}m'$  make at most  $200\varepsilon$  angle with  $-\mathbf{n}_{\tilde{p}}$  (Lemma 6) and hence make an angle of at most  $400\varepsilon$  among themselves. Consider a smaller version of  $D$  by moving its center towards  $p$  till its radius becomes same as that of  $B'$ . Let this new ball be  $D' = B_{\|p-c\|,c}$  (Figure 4). We show that this  $D'$  and hence  $D$  contain  $m$ . We have

$$\begin{aligned} \|m - c\| &\leq \|m - m'\| + \|m' - c\| \\ &\leq \frac{1}{4}(1 - 3\varepsilon^2)f(\tilde{x}) + \varepsilon_4 f(\tilde{x}) + 400\varepsilon r' \\ &= \left(\frac{1}{4} + O(\varepsilon)\right)(1 - 3\varepsilon^2)f(\tilde{x}). \end{aligned}$$

On the other hand, the radius  $\|p - c\|$  of  $D'$  is  $r' = \frac{3}{4}(1 - 3\varepsilon^2)f(\tilde{x})$ . Therefore,  $\|m - c\|$  is smaller than this radius for a sufficiently small  $\varepsilon$ . Hence,

$m$  is in  $D$ . Now we claim that  $y$  and  $m$  are far away and thus  $y$  cannot have any sample point nearby contradicting Lemma 1. Let  $z$  be the point on the medial axis so that  $\|\tilde{x} - m\| = f(\tilde{x}) = \|\tilde{x} - z\|$ . Then,  $\|y - m\| + 2\|\tilde{x} - m\| \geq \|y - z\| \geq f(y)$  giving  $3\|y - m\| \geq f(y)$  or  $\|y - m\| \geq f(y)/3$ . Since  $D$  contains  $m$ , the ball centered at  $y$  with radius  $\|y - m\|$  lies completely inside  $D$  and thus cannot contain any sample point. This means  $y$  cannot have a sample point within  $f(y)/3$  distance, a contradiction to Lemma 1 when  $\varepsilon$  is sufficiently small. This completes the claim that the center of  $B'$  always remain in  $\Omega_I$  while deforming it to  $B''$ .

CLAIM 3.  $B'' \in \mathcal{B}_I$ .

The ball  $B''$  contains four sample points including  $p$  on its boundary. For any of these sample points  $u$ , we have  $\|u - \tilde{u}\| \leq \varepsilon^2 f(\tilde{u})$  by the sampling condition. Therefore, applying Lemma 5 to  $B''$  with points  $p, u \neq p$  and  $\lambda = (\frac{3}{10} - O(\varepsilon))$  we get

$$r'' \geq \frac{\lambda(1 - \varepsilon^2)}{1 + 2\lambda + \varepsilon^2} f(\tilde{u}) \geq (\frac{3}{16} - O(\varepsilon)) f(\tilde{u}).$$

Also we have  $\lambda_u \leq \varepsilon_2 f(\tilde{u})$  from Lemma 2. Thus,  $B''$  is in  $\mathcal{B}$  if

$$\begin{aligned} \frac{(\frac{3}{16} - O(\varepsilon))}{2} &> K\varepsilon_2, \text{ or} \\ 1 &> O(\varepsilon) + 11K\varepsilon_2, \end{aligned}$$

a condition which is satisfied for a sufficiently small  $\varepsilon$ . Since  $m'' \in \Omega_I$  by Claim 2, we have  $B'' \in \mathcal{B}_I$ .

LEMMA CLAIMS: Clearly,

$$r'' \geq r' \geq \frac{3}{4}(1 - 3\varepsilon^2)f(\tilde{x}).$$

This proves (i). Claim 3 proves  $p \in P_I$  which together with Claim 1 give (ii).  $\square$

## 4 Proximity

We aim to prove that the boundary of  $\bigcup \mathcal{B}_I$  is homeomorphic and close to  $\Sigma$ . The proof can be adapted in a straightforward manner for a similar result between the boundary of  $\bigcup \mathcal{B}_O$  and  $\Sigma$ . We define

$$\begin{aligned} S_I &= \text{Boundary of } \bigcup \mathcal{B}_I. \\ S_O &= \text{Boundary of } \bigcup \mathcal{B}_O. \end{aligned}$$

First, we bound the angle between the normals of  $\Sigma$  and the radial directions of the balls in  $\mathcal{B}$  whose boundaries contribute to  $S_I$  and  $S_O$ . Lemma 6 provides this bound at the sample points for some balls. In general, for any point  $x$  in  $S_I$  and any ball  $B$  incident on  $x$ , we will use a result of Amenta, Choi and Kolluri [4] (Lemma 23) to claim a similar result in the next lemma. Although the statement of this lemma is slightly different from that of Lemma 23 [4], the proof can be adapted with only minor modifications.

**Lemma 8** *Let  $x$  be a point in  $S_I$  so that the following conditions hold for a sufficiently small  $\varepsilon$ :*

- (i)  $\|x - \tilde{x}\| = O(\varepsilon)f(\tilde{x})$ ,
- (ii) each point  $y \in \Sigma$  has a sample point within  $O(\varepsilon)f(y)$  distance,
- (iii)  $x$  is in a ball  $B_{r,c} \in \mathcal{B}_I$  so that  $r \geq K\varepsilon f(\tilde{x})$ .

*Then, the angle between  $-\mathbf{n}_{\tilde{x}}$  and the vector  $x\tilde{c}$  is  $O(\sqrt{1/K})$ .*

In the next two lemmas we establish the condition (i) of Lemma 8, that is, we show that each point in  $S_I$  has a nearby point on  $\Sigma$ .

**Lemma 9** *Let  $x$  be a point lying in  $\Omega_O$  where  $x \in S_I$ . Then,  $\|x - \tilde{x}\| \leq \varepsilon_6 f(\tilde{x})$  where  $\varepsilon_6 = \frac{\varepsilon_1}{1 - 2\varepsilon_1}$ .*

PROOF. Let  $x \in B_{r,c}$  where  $B_{r,c} \in \mathcal{B}_I$ . The line segment joining  $x$  and  $c$  must intersect  $\Sigma$  since  $c$  lies in  $\Omega_I$  while  $x$  lies in  $\Omega_O$ . Let this intersection point be  $z$ . We claim that  $\|x - z\| \leq \varepsilon_1 f(z)$ . Otherwise, there is a ball inside  $B_{r,c}$  centering  $z$  and radius at least  $\varepsilon_1 f(z)$ . This ball is empty since  $B_{r,c}$  is empty. This violates Lemma 1 for  $z$ . This means that the closest point  $\tilde{x} \in \Sigma$  to  $x$  has a distance  $\|x - \tilde{x}\| \leq \|x - z\| \leq \varepsilon_1 f(z)$ . We also have  $\|z - \tilde{x}\| \leq 2\|x - z\|$ . Applying the Lipschitz property of  $f()$ , we get the desired bound for  $\|x - \tilde{x}\|$ .  $\square$

**Lemma 10** *Let  $x$  be a point lying in  $\Omega_I$  where  $x \in S_I$ . Then, for a sufficiently small  $\varepsilon$ ,  $\|x - \tilde{x}\| \leq \varepsilon_7 f(\tilde{x})$  where*

$$\varepsilon_7 = (\varepsilon_4 + 300\varepsilon(1 - 3\varepsilon^2)) = O(\varepsilon).$$

PROOF. Let  $y$  be the point in  $\Sigma_{-\varepsilon}$  where the line of  $\mathbf{n}_{\tilde{x}}$  intersects  $\Sigma_{-\varepsilon}$ . Observe that  $x, y$  and  $\tilde{x}$  are collinear. If  $x$  lies between  $\tilde{x}$  and  $y$ , then  $\|x - \tilde{x}\| \leq \varepsilon_3 f(\tilde{x})$  which is no more than  $\varepsilon_7 f(\tilde{x})$ .



So, assume that  $x$  is further away from  $\tilde{x}$  than  $y$  is. Consider a Delaunay ball  $B = B_{r,c} \in \mathcal{B}_I$  guaranteed by Lemma 7. This ball has a sample point  $p \in P$  on the boundary so that  $\|y - p\| \leq \varepsilon_5 f(\tilde{x})$ . Moreover,  $r \geq \frac{3}{4}(1 - 3\varepsilon^2)f(\tilde{x})$ . This ball was obtained by deforming a ball  $B' = B_{r',m'}$  whose boundary passes through  $p$  and a point  $x'$  where  $\|\tilde{x} - x'\| \leq \varepsilon_4 f(\tilde{x})$ . Also  $r' = \frac{3}{4}(1 - 3\varepsilon^2)f(\tilde{x})$ . Focus on the two balls  $B$  and  $B'$  incident to  $p$ . Since  $y$  and  $p$  and hence  $p$  and  $\tilde{x}$  are close, both  $B$  and  $B'$  have radii larger than  $f(\tilde{p})/5$  when  $\varepsilon$  is sufficiently small. By Lemma 6, we obtain that the vectors  $\tilde{p}\tilde{c}$  and  $\tilde{p}m'$  make  $200\varepsilon$  angle with  $-\mathbf{n}_{\tilde{p}}$  and hence make an angle of  $400\varepsilon$  among them.

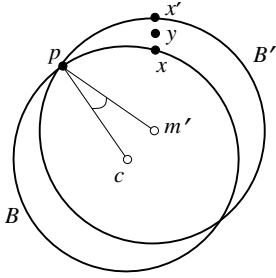


Figure 5: The balls  $B$  and  $B'$  incident to  $p$ . The point  $x'$  is furthest from  $x$  when  $B$  is the smallest possible.

We know that  $B$  has a radius at least as large as  $B'$  (proof of Lemma 7). The points  $x, x', \tilde{x}$  and  $y$  are collinear and  $y$  separates  $x$  and  $x'$ . Further  $x$  cannot lie inside a Delaunay ball. With these constraints, the distance between  $x$  and  $x'$  is the most when  $x$  lies on the boundary of  $B$  and  $B$  is the smallest possible, see Figure 5. This means we can assume that both  $B$  and  $B'$  have the same radius to estimate the worst upper bound on  $\|x - x'\|$ . In that configuration,  $\|x - x'\| \leq \|c - m'\| \leq 400r'\varepsilon$  which is at most  $300\varepsilon(1 - 3\varepsilon^2)f(\tilde{x})$ . Therefore,

$$\begin{aligned} \|x - \tilde{x}\| &\leq \|x - x'\| + \|x' - \tilde{x}\| \\ &\leq (\varepsilon_4 + 300\varepsilon(1 - 3\varepsilon^2))f(\tilde{x}). \end{aligned}$$

□

From Lemma 9 and Lemma 10 we get the following lemma that satisfies the condition (i) of Lemma 8.

**Lemma 11** *For a sufficiently small  $\varepsilon$ , each point  $x$  on  $S_I$  has a point in  $\Sigma$  within  $\varepsilon_8 f(\tilde{x})$  distance where  $\varepsilon_8 = \max\{\varepsilon_6, \varepsilon_7\} = O(\varepsilon)$ .*

The condition (ii) of Lemma 8 follows from Lemma 1.

The condition (iii) of Lemma 8 is established in the next lemma.

**Lemma 12** *Let  $x$  be any point on the boundary of a ball  $B_{r,c} \in \mathcal{B}_I$ , we have  $r \geq (K/2)\varepsilon f(\tilde{x})$  for a sufficiently small  $\varepsilon$ .*

**PROOF.** Suppose the claim is not true. Then, consider a vertex  $p \in P_I$  on the Delaunay ball  $B_{r,c}$ . Since this ball is in  $\mathcal{B}_I$ , we have  $r \geq K\varepsilon f(\tilde{p})$ . Since  $\|x - p\| \leq 2r$ , we have  $\|x - p\| \leq K\varepsilon f(\tilde{x})$  by our assumption. This means  $\|x - \tilde{p}\| \leq K\varepsilon f(\tilde{x}) + \varepsilon^2 f(\tilde{p})$ . Since  $\tilde{x}$  is closer to  $x$  than  $\tilde{p}$ , we have

$$\begin{aligned} \|\tilde{x} - \tilde{p}\| &\leq \|\tilde{x} - x\| + \|x - \tilde{p}\| \\ &\leq 2(K\varepsilon f(\tilde{x}) + \varepsilon^2 f(\tilde{p})). \end{aligned}$$

Using the Lipschitz property of  $f(\cdot)$  we get

$$f(\tilde{x}) \leq \left( \frac{1 + 2\varepsilon^2}{1 - 2K\varepsilon} \right) f(\tilde{p})$$

Therefore by our assumption,

$$r \leq \left( \frac{K}{2} \right) \left( \frac{1 + 2\varepsilon^2}{1 - 2K\varepsilon} \right) \varepsilon f(\tilde{p}).$$

We reach a contradiction if  $\frac{K(1+2\varepsilon^2)}{2(1-2K\varepsilon)} < K$ , a condition which is satisfied for a sufficiently small  $\varepsilon$ . □

## 5 Homeomorphic surface

We have all ingredients to establish a homeomorphism between  $\Sigma$  and  $S_I$ .

**Theorem 1** *The restriction of  $\nu$  to  $S_I$  defines a homeomorphism between  $S_I$  and  $\Sigma$  when  $K$  is sufficiently large and  $\varepsilon$  is sufficiently small.*

**PROOF.** Since  $S_I$  and  $\Sigma$  are both compact we only need to show that  $\nu$  is continuous, one-to-one and onto. The discontinuity of  $\nu$  occurs only at the medial axis of  $\Sigma$ . For any fixed  $K > 0$ , lemmas 7 to 12 hold for a sufficiently small  $\varepsilon$ . In particular, Lemma 11 asserts that each point  $x$  in  $S_I$  is within  $\varepsilon_8 f(\tilde{x})$  distance from  $\tilde{x}$ . Therefore, all points of  $S_I$  are far away from the medial axis when  $\varepsilon$  is sufficiently small. Thus the restriction of  $\nu$  to  $S_I$  is continuous.

To prove that  $\nu$  is one-to-one, assume on the contrary that there are points  $x$  and  $x'$  in  $S_I$  so that  $\tilde{x} = \nu(x) = \nu(x')$ . Without loss of generality assume  $x'$  is further away from  $\tilde{x}$  than  $x$  is. Let  $x \in B_{r,c}$  where  $B_{r,c} \in \mathcal{B}_I$ . The line  $\ell_x$  passing

through  $x$  and  $x'$  is normal to  $\Sigma$  at  $\tilde{x}$ , and according to Lemma 8,  $\ell_x$  makes an angle at most  $\alpha = O(\sqrt{1/K})$  with the vector  $x\tilde{c}$ . Thus, while walking on the line  $\ell_x$  towards the inner medial axis starting from  $\tilde{x}$ , we encounter a segment of length at least  $2r \cos \alpha$  inside  $B_{r,c}$ . By Lemma 11 both  $x$  and  $x'$  are within  $\varepsilon_8 f(\tilde{x})$  distance from  $\tilde{x}$ . We reach a contradiction if  $2r \cos \alpha$  is more than  $\varepsilon_8 f(\tilde{x})$ . Since  $r > (K/2)\varepsilon f(\tilde{x})$  by Lemma 12 and  $\alpha = O(\sqrt{1/K})$ , this contradiction can be reached for a sufficiently small  $\varepsilon$  and a sufficiently large  $K$ . Then,  $x$  and  $x'$  are same.

Now we argue that  $\nu$  is also onto. Since  $S_I$  is a closed, compact surface without boundary and  $\nu$  maps  $S_I$  continuously to  $\Sigma$ ,  $\nu(S_I)$  must consist of closed connected components of  $\Sigma$ . By our assumption,  $\Sigma$  is connected, this means  $\nu(S_I) = \Sigma$  and hence  $\nu$  is onto.  $\square$

## 5.1 Ball separation

In order to apply the previous results, we need to separate the balls in  $\mathcal{B}_I$  from the ones in  $\mathcal{B}_O$ . We achieve this by looking at how deeply the balls intersect. We call two balls in  $\mathcal{B}_I$  ( $\mathcal{B}_O$ ) *neighbors* if their boundaries intersect and a point from this intersection lies in  $S_I$  ( $S_O$  respectively). The neighbor balls in  $\mathcal{B}_I$  or in  $\mathcal{B}_O$  intersect deeply while two balls, one from  $\mathcal{B}_I$  and the other from  $\mathcal{B}_O$ , can have only shallow intersection. We measure the depth of intersection by the angle at which two balls intersect. Let  $x$  be any point where the boundaries of two balls  $B_1$  and  $B_2$  intersect. We say  $B_1$  intersects  $B_2$  at an angle  $\alpha$  if  $\angle(x\tilde{c}_1, x\tilde{c}_2) = \alpha$  where  $c_1$  and  $c_2$  are the centers of  $B_1$  and  $B_2$  respectively.

**Lemma 13** *Any two neighbor balls  $B_1$  and  $B_2$  in  $\mathcal{B}_I$  intersect at an angle  $O(\sqrt{1/K})$  when  $\varepsilon$  is sufficiently small.*

PROOF. Let  $x \in B_1 \cap B_2$  be a point in  $S_I$ . The angle at which  $B_1$  and  $B_2$  intersect at  $x$  is equal to the angle between the vectors  $x\tilde{c}_1$  and  $x\tilde{c}_2$  where  $c_1$  and  $c_2$  are the centers of  $B_1$  and  $B_2$  respectively. By Lemma 8 both  $\angle(-\mathbf{n}_{\tilde{x}}, x\tilde{c}_1)$  and  $\angle(-\mathbf{n}_{\tilde{x}}, x\tilde{c}_2)$  are  $O(\sqrt{1/K})$ . This implies  $\angle(x\tilde{c}_1, x\tilde{c}_2) = O(\sqrt{1/K})$ .  $\square$

**Lemma 14** *For a sufficiently small  $\varepsilon$ , any two balls  $B_1$  and  $B_2$  intersect at an angle more than  $\pi/2 - \arcsin((2/K)(1 + O(\varepsilon)))$  where  $B_1 \in \mathcal{B}_I$  and  $B_2 \in \mathcal{B}_O$ .*

PROOF. The line segment joining the center  $c_1$  of  $B_1$  and the center  $c_2$  of  $B_2$  intersects  $\Sigma$  as  $c_1$  lies in  $\Omega_I$  where  $c_2$  lies in  $\Omega_O$ . Let this intersection point be  $x$ . Without loss of generality, assume that  $x$  lies inside  $B_1$ . Let  $C$  be circle of intersection of  $B_1$  and  $B_2$  and  $d$  be its radius. Clearly,  $d$  is smaller than the distance of  $x$  to the closest sample point as  $B_1$  is empty. This fact and Lemma 1 imply

$$d \leq \varepsilon_1 f(x). \quad (5.5)$$

Next, we obtain a lower bound on the radius of  $B_1$  in terms of  $f(x)$ . Let the segment  $c_1 c_2$  intersect the boundary of  $B_1$  at  $y$ . Lemma 1 implies  $\|x - y\| \leq \varepsilon_1 f(x)$ . This also means  $\|x - \tilde{y}\| \leq 2\varepsilon_1 f(x)$ . By Lipschitz property of  $f(\cdot)$ , we have

$$f(\tilde{y}) \geq (1 - 2\varepsilon_1)f(x).$$

The radius  $r$  of  $B_1$  satisfies (Lemma 12)

$$r > (K/2)\varepsilon f(\tilde{y}) \quad (5.6)$$

$$> (K/2)\varepsilon(1 - 2\varepsilon_1)f(x). \quad (5.7)$$

Combining 5.5 and 5.7 we obtain that, for a point  $z$  on the circle  $C$ ,  $z\tilde{c}_1$  makes an angle at least  $\pi/2 - \arcsin((2/K)(1 + O(\varepsilon)))$  with the plane of  $C$ . The angle at which  $B_1$  and  $B_2$  intersect is greater than this angle.  $\square$

Lemma 13 and 14 say that, for a sufficiently large  $K$ , there is a sufficiently small  $\varepsilon$  so that one can find an angle  $\theta > 0$  where the neighbor balls in  $\mathcal{B}_I$  and  $\mathcal{B}_O$  intersect at an angle less than  $\theta$  and a ball from  $\mathcal{B}_I$  intersects a ball from  $\mathcal{B}_O$  at an angle larger than  $\theta$ . This becomes the basis of separating the balls in  $\mathcal{B}_I$  from the ones in  $\mathcal{B}_O$ .

## 5.2 Algorithm

Now we have all ingredients to design an algorithm that computes a surface homeomorphic to  $\Sigma$ . The algorithm first chooses each Delaunay ball whose radius is bigger than a constant ( $K$ ) times the distance between any sample point  $p$  on its boundary and the  $\kappa$ th nearest sample point of  $p$ . In practice, we take  $\kappa = 3$ . Then, we start walking from an arbitrary big Delaunay ball after marking it. We continue to collect big Delaunay balls that intersect an already marked ball at an angle more than a threshold angle. If the initial ball was an inner (outer) ball chosen from  $\mathcal{B}_I$  ( $\mathcal{B}_O$  respectively), this process will mark all inner balls in  $\mathcal{B}_I$  (outer balls in  $\mathcal{B}_O$  respectively). This is because all balls in  $\mathcal{B}_I$  ( $\mathcal{B}_O$ ) are connected through the neighbor relation as  $S_I$  ( $S_O$  respectively) is so (Theorem 1).

The boundary of the union of the marked balls, or the remaining unmarked big balls can be output as the approximated surface. Alternatively, one can compute a *skin* surface [17] out of these balls that approximates the boundary with a  $C^2$ -smooth surface.

## 6 Interpolating surface

In this section we extend the previous algorithm to produce a piecewise linear surface interpolating through the sample points residing on the inner (or outer) balls. For the proofs we will use  $\kappa = 1$  in this extension though  $\kappa = 3$  works well in practice.

We use the concept of the restricted Delaunay triangulation as described below. The points in  $P_I$  defines a *restricted Voronoi diagram*  $\text{Vor } P_I|_{S_I}$  as the collection of *restricted Voronoi cells*  $\{V_p|_{S_I} = V_p \cap S_I\}$ . Dual to the restricted Voronoi diagram is the *restricted Delaunay triangulation*  $\text{Del } P_I|_{S_I}$ . It is a simplicial complex where  $\sigma \in \text{Del } P_I|_{S_I}$  if and only if  $\sigma$  is the convex hull of a set of vertices  $R \subseteq P$  where  $\bigcap_{q \in R} V_q|_{S_I} \neq \emptyset$ . Notice that one can define the restricted Delaunay triangulation  $\text{Del } P_O|_{S_O}$  similarly.

We compute  $\text{Del } P_I|_{S_I}$ . Equivalently, one may also compute  $\text{Del } P_O|_{S_O}$ . In what follows we consider only  $\text{Del } P_I|_{S_I}$ . Our goal is to show that the  $\text{Del } P_I|_{S_I}$  is homeomorphic to  $S_I$ . This is established by showing that the restricted Voronoi diagram  $\text{Vor } P_I|_{S_I}$  satisfies the *topological ball property* as defined by Edelsbrunner and Shah [19]. This means, in  $\text{Vor } P_I$ , any Voronoi edge intersecting  $S_I$  should intersect it in a single point. Any Voronoi facet intersecting  $S_I$  should intersect it in a topological 1-ball, that is, in a single open curve. Each Voronoi cell should intersect  $S_I$  in a topological disk.

We can show all these three conditions using the technique used to prove the topological ball property for skin surfaces [9]. Although this surface is smooth whereas  $S_I$  is not, we identify the main ingredients in the proofs of Cheng et al. [9] which can be recast in the context of  $S_I$  and thus the rest of the proof can be carried through.

The main ingredients in the proof of Cheng et al. are:

- (i) Each point on the surface in a Voronoi cell  $V_p$  is close to  $p$  with respect to the local feature size at  $p$ .
- (ii) Any two points that are sufficiently close with respect to the local feature sizes have surface normals almost parallel.

- (iii) Each Voronoi edge  $e \in V_p$  intersecting the surface is almost parallel to the normal at  $p$ .
- (iv) Each Voronoi facet  $F \in V_p$  intersecting the surface is parallel to the normal at  $p$ .

The next lemma is the counterpart of (i) for  $S_I$ .

**Lemma 15** *Let  $p \in P_I$  be a sample point in  $S_I$  and  $x$  be any point in  $V_p \cap S_I$ . For a sufficiently small  $\varepsilon$ , we have  $\|p - x\| \leq \varepsilon_9 f(\bar{p})$  where  $\varepsilon_9 = (\varepsilon_3 + \varepsilon_5 + \varepsilon_8) \frac{1 + \varepsilon^2}{1 - \varepsilon_3 - \varepsilon_5 - 2\varepsilon_8} = O(\sqrt{\varepsilon})$ .*

PROOF. Let  $y$  be the closest point of  $x$  on  $\Sigma_{-\varepsilon}$ . It follows from Lemma 7 that  $y$  has a sample point, say  $p'$ , within  $\varepsilon_5 f(\bar{x})$  distance on  $S_I$ . Also,  $\|x - y\| \leq \|x - \bar{x}\| + \|\bar{x} - y\|$ . Lemma 11 gives  $\|x - \bar{x}\| \leq \varepsilon_8 f(\bar{x})$  and Lemma 3 gives  $\|\bar{x} - y\| \leq \varepsilon_3 f(\bar{x})$ . Therefore,

$$\|x - p\| \leq \|x - p'\| \leq \|x - y\| + \|y - p'\| \leq \varepsilon' f(\bar{x})$$

where  $\varepsilon' = \varepsilon_3 + \varepsilon_5 + \varepsilon_8$ . We have

$$\begin{aligned} \|\bar{x} - \bar{p}\| &\leq \|x - p\| + \|x - \bar{x}\| + \|p - \bar{p}\| \\ &\leq (\varepsilon' + \varepsilon_8) f(\bar{x}) + \varepsilon^2 f(\bar{p}). \end{aligned}$$

Using the Lipschitz property of  $f(\cdot)$  we get

$$f(\bar{x}) \leq \frac{1 + \varepsilon^2}{1 - \varepsilon' - \varepsilon_8} f(\bar{p}).$$

Using the above inequality in the relation  $\|x - p\| \leq \varepsilon' f(\bar{x})$  we get the desired result.  $\square$

The next lemma is the counterpart of (ii) for  $S_I$ .

**Lemma 16** *Let  $p$  and  $q$  be any two points in  $S_I$  where  $\|\bar{p} - \bar{q}\| \leq \delta f(\bar{p})$  where  $\delta \leq 1/4$ . Let  $B_{r,c}$  and  $B'_{r',c'}$  be two balls in  $\mathcal{B}_I$  containing  $p$  and  $q$  respectively on their boundaries. Then,  $\angle \vec{p}\bar{c}, \vec{q}\bar{c}' = O(\sqrt{\frac{1}{K}} + \delta)$  when  $\varepsilon$  is sufficiently small. .*

PROOF. By Lemma 8, we have  $\angle \mathbf{n}_{\bar{p}}, \vec{p}\bar{c}$  and  $\angle \mathbf{n}_{\bar{q}}, \vec{q}\bar{c}'$  are  $O(\sqrt{\frac{1}{K}})$ . Also, an immediate corollary of Lemma 2 of Amenta and Bern [2] is that  $\angle \mathbf{n}_{\bar{p}}, \mathbf{n}_{\bar{q}} = O(\delta)$ . The claim follows.  $\square$

The following lemma is used to claim that the triangles in  $\text{Del } P_I|_{S_I}$  lie almost flat to the surface  $S_I$ . This in turn will imply (iii). The normal  $\mathbf{n}_t$  of a triangle  $t$  in  $\text{Del } P_I|_{S_I}$  is assumed to be oriented outward.

**Lemma 17** *Let  $t$  be a triangle and the following conditions hold for each vertex  $q$  of  $t$ .*

- (i)  $q$  lies within  $\varepsilon^2 f(\tilde{q})$  distance from  $\Sigma$ ,
- (ii)  $q$  is more than  $\varepsilon f(\tilde{q})$  distance away from all other vertices of  $t$ ,
- (iii) the circumradius of  $t$  is at most  $\lambda f(\tilde{q})$ .

Then, for  $\lambda > \varepsilon^2$ ,  $\angle \mathbf{n}_t, \mathbf{n}_{\tilde{q}} = O(\lambda)$  where both  $\lambda$  and  $\varepsilon$  are sufficiently small.

PROOF. Let  $p$  be the vertex of  $t$  subtending the largest angle. First, we prove that there are two balls of radius at least  $\frac{f(\tilde{p})}{12}$  being tangent at  $p$  and with centers on the line of  $\mathbf{n}_{\tilde{p}}$  in  $\Omega_I$  and  $\Omega_O$  respectively.

Consider a feature ball  $B = B_{m, (1-3\varepsilon^2)f(\tilde{p})}$  with the center in  $\Omega_I$ . This ball is empty and therefore does not contain any vertex of  $t$ . Consider a ball  $D$  with the center  $p$  and radius  $\varepsilon f(\tilde{p})$ . This ball also does not contain any vertex of  $t$  by the condition (ii). Let  $C$  be the circle of intersection of the boundaries of  $B$  and  $D$ . Let  $B' = B_{r, w}$  be the ball whose boundary passes through  $C$  and  $p$  (Figure 6). No vertex of  $t$  lies inside  $B'$  as  $B' \subset B \cup D$  and both  $B$  and  $D$  are empty of the vertices of  $t$ . We claim that  $r \geq f(\tilde{p})/12$  when  $\varepsilon$  is sufficiently small.

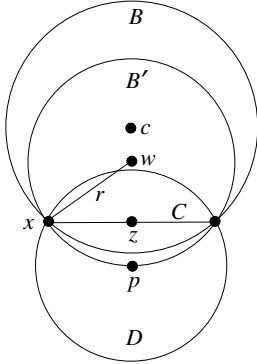


Figure 6: Illustration for Lemma 17.

Let  $x$  be any point on the circle  $C$  whose center is  $z$ . The radius  $R$  of  $B$  is equal to  $(1 - 3\varepsilon^2)f(\tilde{p})$ . So,  $\|x - p\| = \frac{\varepsilon}{1-3\varepsilon^2}R$ . The distance  $d(p, B) \leq \|p - \tilde{p}\| + d(\tilde{p}, B)$ . We have  $\|p - \tilde{p}\| \leq \varepsilon^2 f(\tilde{p})$ , and  $d(\tilde{p}, B) \leq 3\varepsilon^2 f(\tilde{p})$ . So,

$$d(p, B) \leq 4\varepsilon^2 f(\tilde{p}) \leq \frac{4\varepsilon^2}{1 - 3\varepsilon^2}R \leq 5\varepsilon^2 R$$

for a sufficiently small  $\varepsilon$ . It can be proved that the above fact with the constraint that the radius of  $D$  is  $\varepsilon f(\tilde{p})$  gives

$$r \geq \frac{R}{9} = \frac{f(\tilde{p})(1 - 3\varepsilon^2)}{9} \geq \frac{f(\tilde{p})}{12}$$

when  $\varepsilon$  is sufficiently small.

Applying the above argument to the other feature ball  $B_{m', (1-3\varepsilon^2)f(\tilde{p})}$  where  $m' \in \Omega_O$  we get another empty ball  $B''$  with radius at least  $\frac{f(\tilde{p})}{12}$  touching  $p$ . The centers of both  $B'$  and  $B''$  lie on the line of the normal  $\mathbf{n}_{\tilde{p}}$ . Notice that both  $B'$  and  $B''$  meet at a single point  $p$ . Shrink both  $B'$  and  $B''$  keeping them tangent at  $p$  till their radius is equal to  $f(\tilde{p})/12$ . Now applying a result of Amenta et al. [3] to the balls  $B'$ ,  $B''$  and the triangle  $t$  we can conclude that the acute angle between the lines of  $\mathbf{n}_t$  and  $\mathbf{n}_{\tilde{p}}$  is at most  $O(\lambda)$ . If  $\lambda$  is sufficiently small, this angle is less than  $\frac{\pi}{2}$ . This implies that the upper bound of  $O(\lambda)$  also holds for the oriented normals, i.e.,

$$\angle \mathbf{n}_t, \mathbf{n}_{\tilde{p}} = O(\lambda).$$

Now, consider any vertex  $q$  of  $t$ . Since the circumradius of  $t$  is no more than  $\lambda f(\tilde{q})$ ,  $\|p - q\| \leq 2\lambda f(\tilde{q})$ . We have  $\|\tilde{p} - \tilde{q}\| \leq 2(2\lambda + \varepsilon^2)f(\tilde{q}) \leq 6\lambda f(\tilde{q})$  for  $\varepsilon^2 < \lambda$ . Then, by a result of Amenta and Bern [2]  $\angle \mathbf{n}_{\tilde{p}}, \mathbf{n}_{\tilde{q}} = O(\lambda)$  provided  $\lambda$  is sufficiently small. Therefore,

$$\angle \mathbf{n}_t, \mathbf{n}_{\tilde{q}} = O(\lambda).$$

□

We can use the above lemma to establish that the triangles in  $\text{Del } P_I|_{S_I}$  have normals almost parallel to the normals of  $S_I$ .

**Lemma 18** *Let  $pqr$  be any triangle in the restricted Delaunay triangulation  $\text{Del } P_I|_{S_I}$  where  $p$  is on the boundary of  $B_{r, c} \in \mathcal{B}_I$ . Then, for a sufficiently small  $\varepsilon$ ,  $\angle -\mathbf{n}_{pqr}, \tilde{p}\tilde{c} = O(\frac{1}{\sqrt{R}} + \sqrt{\varepsilon})$  where  $\mathbf{n}_{pqr}$  is the normal of  $pqr$ .*

PROOF. The triangle  $pqr$  satisfies the conditions (i) and (ii) of Lemma 17 by our sampling conditions ( $\kappa = 1$ ). Lemma 15 implies that  $pqr$  has a circumradius at most  $\varepsilon_9 f(\tilde{p}) = O(\sqrt{\varepsilon})f(\tilde{p})$ . Plugging this for  $\lambda$  in Lemma 17, we get that

$$\angle \mathbf{n}_{pqr}, \mathbf{n}_{\tilde{p}} = O(\sqrt{\varepsilon}).$$

Also, from Lemma 8 we have

$$\angle -\mathbf{n}_{\tilde{p}}, \tilde{p}\tilde{c} = O(\sqrt{\frac{1}{K}}).$$

The above two facts together give the desired result. □

Lemma 18 implies that the dual Voronoi edge of  $pqr$  is almost parallel to the normal at  $p$  on the

boundary of a big Delaunay ball in  $\mathcal{B}_I$ . This is the counterpart of condition (iii) listed before.

Similar to triangles, small edges in  $\text{Del } P_I|_{S_I}$  also lie almost parallel to  $\Sigma$  and hence to  $S_I$ .

**Lemma 19** *Let  $pq$  be an edge in the restricted Delaunay triangulation  $\text{Del } P_I|_{S_I}$  where  $p$  is on the boundary of  $B_{r,c} \in \mathcal{B}_I$ . Then,  $\angle \vec{p}\vec{q}, \vec{p}\vec{c} = \frac{\pi}{2} - O(\frac{1}{\sqrt{K}} + \sqrt{\varepsilon})$ .*

**PROOF.** Consider the two balls  $B'$  and  $B''$  meeting at the vertex  $q$  as in the proof of Lemma 17. These two balls have radius  $r \geq f(\tilde{q})/12$ . Since these two balls cannot contain the vertex  $p$  inside,  $qp$  makes the smallest angle with the normal  $\mathbf{n}_{\tilde{q}}$  when  $p$  is on the boundary of either  $B'$  or  $B''$ . In either case the angle is more than  $\frac{\pi}{2} - \arcsin \frac{\|p-q\|}{2r} = \frac{\pi}{2} - O(\sqrt{\varepsilon})$ . Now apply Lemma 8 to get the desired bound on  $\angle \vec{p}\vec{q}, \vec{p}\vec{c}$ .  $\square$

Using the above lemmas one can carry out the proof that  $\text{Vor } P_I|_{S_I}$  satisfies the topological ball property. We have the next theorem.

**Theorem 2**  *$\text{Del } P_I|_{S_I}$  is homeomorphic to  $\Sigma$ , when  $K$  is sufficiently large  $\varepsilon$  is sufficiently small. Further, each point  $x$  in  $\text{Del } P_I|_{S_I}$  has a point in  $\Sigma$  within  $O(\sqrt{\varepsilon})f(\tilde{x})$  distance, and conversely, each point  $x$  in  $\Sigma$  has a point in  $\text{Del } P_I|_{S_I}$  within  $O(\sqrt{\varepsilon})f(x)$  distance.*

## 6.1 Implementation

The theory for computing the interpolating surface implies the following two phases. First, the algorithm collects the points on the outer (or inner) balls as described before. Next, it computes a surface interpolating the collected points by using the restricted Delaunay triangulation of the filtered point set with respect to the boundary of the union of the outer (or inner) Delaunay balls. In implementation we filtered the point set as described. However, for the second phase we did not compute the restricted Delaunay triangulation. Instead, we used a surface reconstruction software called TIGHT COCONE [25] to reconstruct the surface from the filtered point set. We did this to avoid the computations for the restricted Delaunay triangulations. Naming after the COCONE algorithm for noise-free point clouds, we call this algorithm ROBUST COCONE.

We used CGAL [26] for the Delaunay triangulation and other geometric primitives. We took  $K = 0.5$ ,  $\kappa = 3$  for choosing the big Delaunay

balls and  $\theta = 15^\circ$  for separating outer balls. We experimented with several noisy data sets. Also, we considered noise-free point sets just to illustrate that ROBUST COCONE is also effective when there is no noise. Two examples of noise-free cases are shown in Figure 7. The output for noisy cases are shown in Figure 8.

ROBUST COCONE as implemented applies TIGHT COCONE on the filtered point set. We compare the results of this implementation with the ones obtained by applying TIGHT COCONE [25] directly on the input. ROBUST COCONE performs much better on noisy data where noise is reasonably high. One aspect of the algorithm is that it tends to produce much less non-manifold vertices and edges as depicted in the BUNNY model. Also, the algorithm is able to reconstruct the surface where the input point set samples the volume as depicted in the FEMUR model.

## 7 Conclusions

In this paper we presented a provable algorithm for surface reconstruction from noisy point cloud data. The noise model is reasonable. The input point set has to be dense with respect to the local feature sizes to capture the features of the surface. Its scatter around the surface has to be bounded to achieve any sort of theoretical guarantees. Furthermore, as points may collaborate to form arbitrary patterns such as a dense sampling of a spurious surface, some form of locally uniform sampling condition is necessary. We have incorporated these three conditions into our noise model. In order to have a less restrictive noise model, it seems that some sacrifice in the guarantees or some assumption in the algorithms have to be made.

The sampling condition (ii) requires a quadratic dependence ( $\varepsilon^2$ ) on the sampling parameter. One can relax this condition to be linearly dependent on  $\varepsilon$  by trading off the normal approximation guarantee. Lemma 6 will give an  $O(\sqrt{\varepsilon})$  approximation to normals at the sample points. This will in turn give an  $O(\sqrt{\varepsilon})f(\tilde{x})$  bound on the distances between any point  $x$  in  $S_I$  and  $\tilde{x}$  in  $\Sigma$  in Lemma 10. As a consequence Lemma 8 will provide an  $O(\frac{1}{\sqrt{K\sqrt{\varepsilon}}})$  approximation for the normals which will mean that  $K\sqrt{\varepsilon}$  has to be large, or  $K$  has to be large, say  $\Omega(\frac{1}{\varepsilon})$ , to have a good normal approximations. This observation suggests that larger the noise amplitude, the bigger the parameter  $K$  should be for choosing big Delaunay balls. It would be interesting to see what kind of other trade offs can be achieved

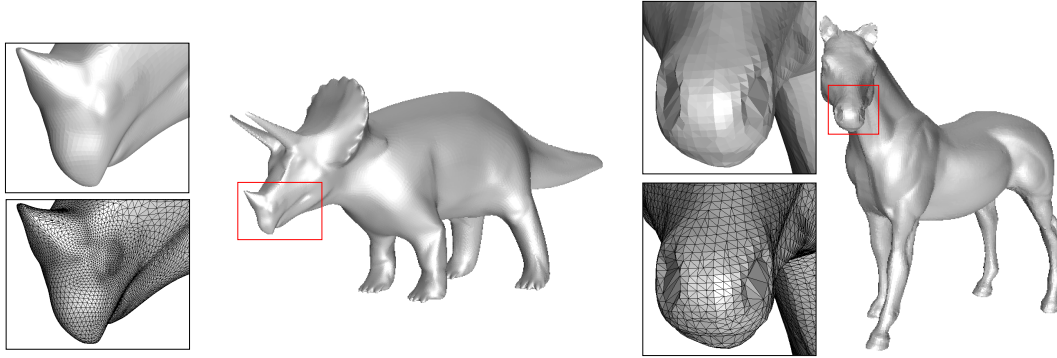


Figure 7: Smooth Surface Reconstruction by Robust Cocone

between the guarantees and the noise models.

We have assumed that  $\Sigma$  is connected. All definitions and proofs can be easily extended to the case when  $\Sigma$  has multiple components. However, it is not clear how to extend the labeling algorithm to separate the balls on two sides of a component of  $\Sigma$  when it has multiple components. It is important that all the big Delaunay balls on one side remain connected through the neighbor relation as defined in section 5.1. When  $\Sigma$  has multiple components, we cannot appeal to Theorem 1 to claim the connectedness among the big Delaunay balls since the surface  $S_I$  may not be connected as  $\Sigma$  is not. This is also a bottleneck for the power crust algorithm [4]. It would be interesting to devise a labeling algorithm which can handle multiple components with guarantee.

The algorithm requires two Delaunay triangulation computations, one for the filtering phase and another for the surface reconstruction phase. Although it has been shown that the Delaunay triangulation has near-linear complexity [5] for locally uniform samples on smooth surfaces, it would be interesting to see if similar bound holds for noisy samples.

Our algorithm requires that the sampled surface have no boundary. It is not clear how the algorithm should be adapted for surfaces with boundary. Reconstruction of surfaces with boundaries from noiseless point samples have been addressed [13]. However, noise together with boundaries pose a difficult challenge.

Although the output of ROBUST COCONE has the exact topology and approximate geometry of the sampled surface, our experiments show that, sometimes it contains undesirable undulations. In most applications this surface needs to be smoothed. There are several mesh smoothing tech-

niques known in graphics. We have experimented with the idea of merging one such smoothing technique called MLS smoothing [1, 23] with the concepts used in ROBUST COCONE; see [14, 16] for details.

## References

- [1] M. Alexa, J. Behr, D. Cohen-Or, S. Fleishman, D. Levin and C. Silva. Point set surfaces. *Proc. IEEE Visualization* (2001), 21–28.
- [2] N. Amenta and M. Bern. Surface reconstruction by Voronoi filtering. *Discr. Comput. Geom.* **22** (1999), 481–504.
- [3] N. Amenta, S. Choi, T. K. Dey and N. Leekha. A simple algorithm for homeomorphic surface reconstruction. *Internat. J. Comput. Geom. & Applications* **12** (2002), 125–141.
- [4] N. Amenta, S. Choi and R. K. Kolluri. The power crust, union of balls, and the medial axis transform. *Comput. Geom.: Theory Applications* **19** (2001), 127–153.
- [5] D. Attali, J.-D. Boissonnat and A. Lieutier. Complexity of the Delaunay triangulation of points on surfaces: the smooth case. *Proc. 19th Annu. Sympos. Comput. Geom.* (2003), 201–210.
- [6] F. Bernardini, J. Mittleman, H. Rushmeier, C. Silva and G. Taubin. The ball-pivoting algorithm for surface reconstruction. *IEEE Trans. Vis. Comput. Graphics* **5**, 349–359.
- [7] J. D. Boissonnat. Geometric structures for three dimensional shape representation, *ACM Transact. Graphics* **3** (1984), 266–286.

- [8] J. D. Boissonnat and F. Cazals. Smooth surface reconstruction via natural neighbor interpolation of distance functions. *Proc. 16th. Annu. Sympos. Comput. Geom.* (2000), 223–232.
- [9] H.-L. Cheng, T. K. Dey, H. Edelsbrunner and J. Sullivan. Dynamic skin triangulation. *Discrete Comput. Geom.* **25** (2001), 525–568.
- [10] S.-W. Cheng, S. Funke, M. Golin, P. Kumar, S.-H. Poon and E. Ramos. Curve reconstruction from noisy samples. *Proc. 19th Annu. Sympos. Comput. Geom.* (2003), 302–311.
- [11] S.-W. Cheng and S.-H. Poon. Surface reconstruction from noisy samples. *Theoretical Computer Science Group Research Report, HKUST-TCSC-2004-05*, 2004.
- [12] T. K. Dey and J. Giesen. Detecting under-sampling in surface reconstruction. *Proc. 17th Annu. Sympos. Comput. Geom.* (2001), 257–263.
- [13] T. K. Dey and S. Goswami. Tight cocone: A watertight surface reconstructor. *J. Computing Informat. Sci. Engin.* **13** (2003), 302–307.
- [14] T. K. Dey and S. Goswami. Smoothing noisy point cloud data with Delaunay preprocessing and MLS. *Tech. Rep. OSU-CISRC-3/04-TR17*, Dept. of CSE, The Ohio State University, 2004.
- [15] T. K. Dey, S. Funke and E. A. Ramos. Surface reconstruction in almost linear time under locally uniform sampling condition. *17th European Workshop Comput. Geom.* (2001), Berlin, Germany.
- [16] T. K. Dey and J. Sun. Adaptive MLS surfaces for reconstruction with guarantees. *Proc. Eurographics Sympos. Geom. Processing* (2005), 43–52.
- [17] H. Edelsbrunner. Deformable smooth surface design. *Discrete Comput. Geom.* **21** (1999), 87–115.
- [18] H. Edelsbrunner. Surface reconstruction by wrapping finite point sets in space. *Ricky Pollock and Eli Goodman Festschrift*, eds. B. Aronov, S. Basu, J. Pach and M. Sharir, Springer-Verlag, 379–404.
- [19] H. Edelsbrunner and N. Shah. Triangulating topological spaces. *Proc. 10th ACM Sympos. Comput. Geom.* (1994), 285–292.
- [20] J. Giesen and M. John. The flow complex: A data structure for geometric modeling. *Proc. 14th. Annu. ACM-SIAM Sympos. Discrete Algorithms* (2003), 285–294.
- [21] H. Hoppe, T. DeRose, T. Duchamp, J. McDonald and W. Stuetzle. Surface reconstruction from unorganized points. *SIGGRAPH 92* (1992), 71–78.
- [22] R. K. Kolluri, J. R. Shewchuk and J. F. O’Brien. Watertight spectral surface reconstruction. *Proc. Sympos. Geometry Process.* (2004).
- [23] D. Levin. The approximation power of moving least-squares. *Math. Computation* **67** (1998), 1517–1531.
- [24] N. J. Mitra, A. Nguyen and L. Guibas. Estimating surface normals in noisy point cloud data. *Internat. J. Comput. Geom. Appl.*, to appear.
- [25] [www.cse.ohio-state.edu/~tamaldey/cocone.html](http://www.cse.ohio-state.edu/~tamaldey/cocone.html)
- [26] [www.cgal.org](http://www.cgal.org)

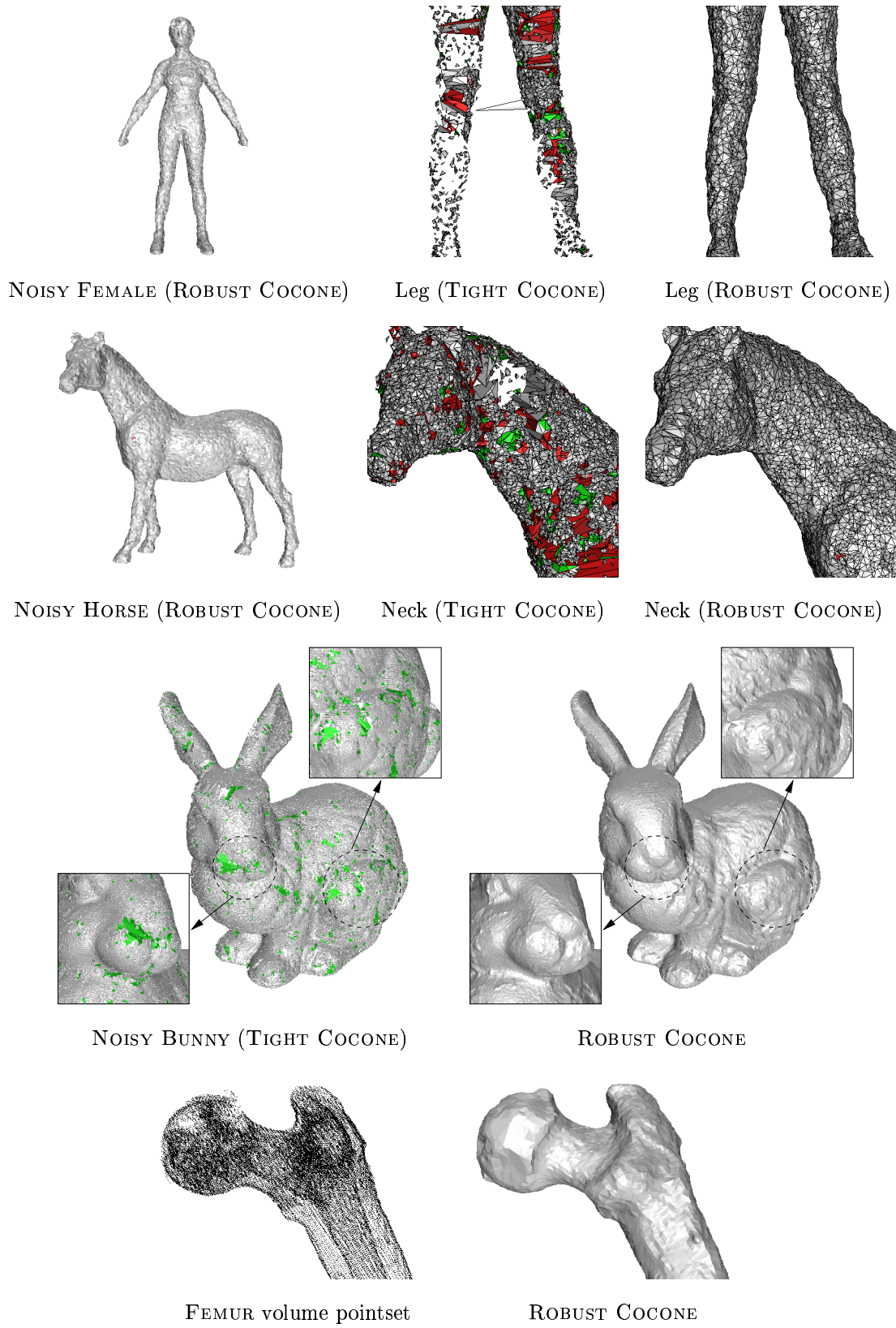


Figure 8: Results: Reconstruction by ROBUST COCONE and its comparison to TIGHT COCONE.